Available online www.ejaet.com

European Journal of Advances in Engineering and Technology, 2024, 11(8):117-136

Research Article ISSN: 2394 - 658X

Two-dimensional Wind and Pressure Fields Generation for Typhoon Gaemi (July 2024) in the Philippines

Md Akhtaruzzaman Sarker (PhD)

Technical Director, Royal HaskoningDHV,
Westpoint, Peterborough Business Park, Lynch Wood,
Peterborough PE2 6FZ, United Kingdom.
E-mail: zaman.sarker@rhdhv.com

ABSTRACT

Typhoons (also known as cyclones or hurricanes) cause significant loss of life and damage to properties, marine facilities and ecosystems. Typhoon modelling results are used for deriving robust design conditions for coastal and marine structures and facilities. These are also used for emergency planning and decision-making to estimate potential loss of life, damage to properties and marine facilities and to develop rescue and mitigation measures and plan clean-up operations. Typhoon Gaemi, known in the Philippines as Super Typhoon Carina, was a powerful tropical cyclone that impacted East China after severely affecting Taiwan and the Philippines in late July 2024. This paper has focused to Typhoon Gaemi as less information is available on this event. Raw data (such as track, wind speed, pressure, and radius of maximum wind speed) were obtained from IBTrACS. Two-dimensional wind and pressure fields along the entire track were then generated using the Cyclone Wind Generation Tool developed by DHI. Two-dimensional wind and pressure fields at selected locations along the track are presented in this paper. Time-series wind speed and pressure over the entire passage of the typhoon are also provided at these selected locations. These wind and pressure fields will be useful for numerical modelling of waves and surge. Structural design considerations and typhoon risk reduction measures are also described in this paper. The methodology described in this paper for generating wind and pressure fields from Typhoon Gaemi could also be applied for other typhoons around the world.

Keywords: Natural hazards, cyclones, hurricanes, typhoons, Typhoon Gaemi, port development, Royal HaskoningDHV.

INTRODUCTION

Formation of Typhoons

Tropical cyclones (also known as hurricanes or typhoons) are associated with warm and moist air and hence they form only over warm ocean waters near the equator (within latitude 30° north and south). They need some favourable conditions to form such as a) warm sea surface temperature b) large convective instability c) low level positive vorticity d) weak vertical wind shear of horizontal wind and e) Coriolis force. Warm ocean waters of at least 27°C throughout a depth of about 50m from sea surface is required for cyclone formation.

The warm and moist air rises causing an area of lower pressure beneath. Cooler air moves into the lower pressure area and becomes warm and moist and rises too. When the warm and moist air rises, it cools down and forms clouds. The entire system of clouds and winds spins and grows and is fed by ocean's heat and evaporated water continuously. Cyclones that form north of the equator spin counterclockwise whereas cyclones south of the equator spin clockwise due to the difference in Earth's rotation on its axis.

Storm surges from cyclones are generated due to an interaction between air and water. The atmosphere forces the water body and consequently oscillations are generated in the water body with periods ranging from a few minutes to a few days. A cyclone becomes deadly by causing inundation along the coastline if the maximum surge coincides with a high astronomical tide. There are essentially two major forcing factors when a weather system moves over a water body. 1) Atmospheric pressure gradient normal to the sea surface. This is known as "inverse barometer effect" or "static amplification" or "the static part of the storm surge". A decrease of one hectopascal (hPa) in the

atmospheric pressure raises the sea level by one centimeter (cm). This static part has only about 5-15% contribution in the magnitude of a surge. 2) The dominant factor, known as "dynamic amplification", is caused by the tangential wind stress (associated with the wind field of the weather system) acting over the sea surface which pushes the water towards the coast resulting to a pile-up of water at the coast.

The Saffir-Simpson Hurricane Wind Scale

The well-known Saffir-Simpson Hurricane Wind Scale [1] is designed to help determine wind hazards of an approaching hurricane easier for emergency officials. The scale is assigned five categories with Category 1 assigned to a minimal hurricane and Category 5 to a worst-case scenario. The Saffir-Simpson Scale classifying hurricane Category 1 to 5 is given in Table 1 [1]. Conditions for tropical depression and tropical storm are also provided in the table.

Table 1: Saffir-Simpson Hurricane Classification [1]

Storm type	Category	Minimum pressure (hPa, mb)	1-minute maximum sustained wind speed				Surge (m)	Damage
			knots	mph	km/h	m/s		
Tropical Depression	TD	-	< 34	<39	< 63	0-17	0	-
Tropical Storm	TS	-	34 – 63	39 – 73	63 – 118	18-32	0-0.9	-
Hurricane	1	> 980	64 – 82	74 – 95	119 – 153	33-42	1.0-1.7	Minimal
Hurricane	2	965 – 980	83 – 95	96 – 110	154 – 177	43-49	1.8-2.6	Moderate
Hurricane	3	945 – 965	96 – 113	111 – 130	178 – 210	50-58	2.7-3.8	Extensive
Hurricane	4	920 – 945	114 – 135	131 - 155	211 - 250	59-69	3.9-5.6	Extreme
Hurricane	5	< 920	> 135	> 155	> 250	>70	>5.7	Catastrophic

Damages from Typhoons

Typhoons are associated with high-pressure gradients and consequently generate strong winds, torrential rain and storm surges at landfall making these one of Earth's most destructive natural phenomena. The destruction from a tropical cyclone depends on its intensity, size and location. Very strong winds may damage installations, dwellings, transportation and communication systems, trees etc. and cause fires resulting in considerable loss of life and damage to property and ecosystems. Cyclones also impose significant risks during construction and operation of seaports and other marine structures and facilities.

Typhoons have been responsible for the deaths of about 1.9 million people worldwide during the last two centuries. It is estimated that 10,000 people per year perish due to tropical cyclones [2]. Bangladesh is especially vulnerable to tropical cyclones with around 718,000 deaths from them in the past 50 years [3]. The deadliest tropical cyclone in Bangladesh was Cyclone Bhola (1970), which had a death toll of at least 300,000 [4] possibly as many as 500,000 [5, 6]. An estimated over 138,000 people were killed [7] with an equal number of injured [8] and about 13.4 million people were affected [8] by the 1991 Cyclone in Bangladesh.

During the 50 years since Cyclone Bhola, 1942 disasters were attributed to tropical cyclones which killed 779,324 people and caused US$ 1,407.6 billion in economic losses with an average of 43 deaths and US$ 78 million in damages every day [9].

Maximum damages from a cyclone occur if landfall takes place at high tide. There was a severe cyclone in the Bay of Bengal in October 1960 which claimed only over 5,000 lives [10] although the strength of this cyclone was like that of Cyclone Bhola (November 1970). The significant difference in fatalities is because the November 1970 cyclone crossed the coast at high tide while the October 1960 storm moved onshore at low tide [11].

Benefits from Typhoons

Despite their devastating effects, tropical cyclones are essential features of the Earth's atmosphere as they bring rain to dry areas and transfer heat and energy from the equator to the cooler regions nearer the poles.

Major Typhoons in the Philippines

The Philippines is a typhoon-prone country with approximately 20 typhoons each year. Typhoons regularly form in the Philippine Sea and less regularly in the West Philippine Sea. June to September are the most active months and August being the month with the most activity. Each year at least ten typhoons are expected to hit the island nation with five expected to be destructive and powerful [12]. The Philippines is the most exposed country in the world to tropical storms [13].

Typhoons typically make an east-to-west route in the Philippines heading north or west due to the Coriolis force effect. As a result landfalls occur in the regions of the country that face the Pacific Ocean especially Eastern

Visayas, Bicol Region, and northern Luzon whereas Mindanao is largely free of typhoons [13]. Typhoon activity in the Philippines reaches to a minimum in May before increasing steadily to June and spiking from July to September with August being the most active month for tropical cyclones. Activity reduces significantly in October [14]. Climate change is likely to worsen the situation with extreme weather events including typhoons posing various risks and threats to the Philippines [15].

The Philippines was hit by 565 natural disasters since 1990 that claimed the lives of more than 70,000. Millions are left homeless by each extreme weather event, with their livelihoods destroyed and clean water and food in short supply. Eachyear an average of 20 typhoons make landfall leaving affected communities repeatedly grappling with hunger, disease, and chronic poverty [16].

Figure 1 shows the tracks of tropical cyclones worldwide (1945–2006) [17]. The Philippines is under the red and yellow tracks (which indicates stronger intensity) northeast of Borneo in the figure. Table 2 shows the deadliest, costliest, and wettest typhoons (top ten of each category) in the Philippines [18].

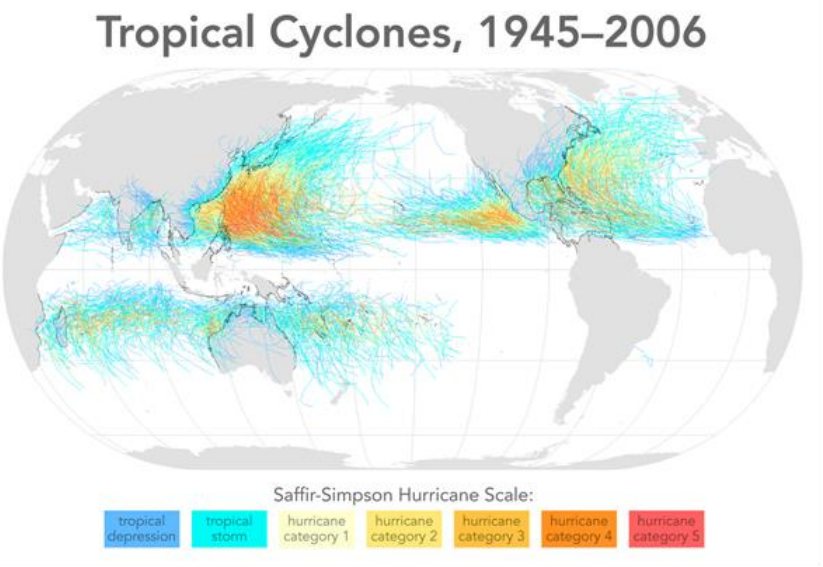

Figure 1: *Tracks of tropical cyclones worldwide (1945–2006) [17]*

The table suggests that the deadliest typhoon was Typhoon Yolanda (Haiyan) in 2013 killing 6,300 [19] as reported in [18]. This typhoon was also the costliest event with an estimated damage of $2.2 billion [20] as reported in [18]. The wettest typhoon was the July 1911 typhoon with total precipitation of 2,210mm in Baguio [21] as reported in [18]. The table suggests that the deadliest typhoons are not necessarily the costliest or the wettest. Information in this section was obtained from Wikipedia [18].

Table 2: Deadliest, costliest, and wettest typhoons in the Philippines [18]

No.	Storm	Season	Fatalities	Damage (USD)	Precipitation	
					mm	Location
1	Yolanda (Haiyan)	2013	6,300	2.2 billion	-	-
2	Uring (Thelma)	1991	5,101–8,000	-	-	-
3	Pablo (Bopha)	2012	1,901	1.06 billion	-	-
4	Angela	1867	1,800	-	-	-
5	Winnie	2004	1,593	-	-	-
6	October 1897	1897	1,500	-	-	-
7	Nitang (Ike)	1984	1,426	-	-	-
8	Reming (Durian)	2006	1,399	-	-	-
9	Frank (Fengshen)	2008	1,371	-	-	-
10	Washi (Sendong)	2011	1,257	-	-	-
11	Odette (Rai)	2021	-	1.02 billion	-	-
12	Glenda (Rammasun)	2014	-	771 million	-	-
13	Ompong (Mangkhut)	2018	-	627 million	-	-
14	Pepeng (Parma)	2009	-	581 million	1,854	Baguio
15	Ulysses (Vamco)	2020	-	418 million	-	-
16	Rolly (Goni)	2020	-	369 million	-	-
17	Pedring (Nesat)	2011	-	356 million	-	-
18	Paeng (Nalgae)	2022	-	321 million	-	-
19	July 1911 cyclone	1911	-	-	2,210	Baguio

20	Trining (Carla)	1967	-	-	1,216	Baguio
21	Iliang (Zeb)	1998	-	-	1,116	La Trinidad, Benguet
22	Feria (Utor)	2001	-	-	1,086	Baguio
23	Lando (Koppu)	2015	-	-	1,078	Baguio
24	Igme (Mindulle)	2004	-	-	1,013	-
25	Dante (Kujira)	2009	-	-	902	-
26	September 1929 typhoon	1929	-	-	880	Virac, Catanduanes
27	Openg (Dinah)	1977	-	-	870	Western Luzon

The Present Study

Typhoon Gaemi, known in the Philippines as Super Typhoon Carina, was a powerful tropical cyclone that impacted East China after severely affecting Taiwan and the Philippines in late July 2024. This paper has focused to Typhoon Gaemi as less information is available on this event.

Raw data (such as track, wind speed, pressure, and radius of maximum wind speed) were obtained from the International Best Track Archive for Climate Stewardship (IBTrACS) [22]. Two-dimensional wind and pressure fields along the entire track were then generated using the Cyclone Wind Generation Tool developed by DHI [23]. Two-dimensional wind and pressure fields at selected locations along the track are presented in this paper. Time-series wind speed and pressure over the entire passage of the typhoon are also provided at these selected locations.

The wind and pressure fields presented in this paper will be useful for numerical modelling of waves and surge. Structural design considerations and cyclone risk reduction measures are also described in this paper. The methodology described in this paper for generating wind and pressure fields from Typhoon Gaemi could also be applied for other typhoons around the world.

TYPHOON GAEMI (17-27 JULY 2024)

Formation of Typhoon Gaemi

Typhoon Gaemi (known in the Philippines as Super Typhoon Carina) was a powerful and destructive tropical cyclone that impacted East China after severely affecting Taiwan and the Philippines in late July 2024. The origin of Typhoon Gaemi can be traced back to 17 July, when the Japan Meteorological Agency (JMA) [24] reported that a low-pressure area had formed east of Palau. Gaemi formed as a tropical depression east of Palau on 19 July. The Joint Typhoon Warning Center (JTWC) [25] issued a tropical cyclone formation alert for the system on 19 July due to its rapidly consolidating broad low-level circulation centre. The system then intensified into a severe tropical storm due to being in a conducive environment for development on 21 July. Around 00:00 UTC on 22 July, the JMA reported that Gaemi had intensified into a typhoon due to good upper-level outflow, warm sea surface temperatures, and high ocean heat content. The storm then turned north-northwestward, along the western periphery of a subtropical ridge. The JTWC upgraded Gaemi to minimal typhoon-equivalent status around 21:00 UTC that day. After undergoing an eyewall replacement cycle and developing a pinhole eye, Gaemi rapidly intensified and peaked at Category 4-equivalent intensity on the Saffir-Simpson scale [1] at 21:00 UTC on 23 July, with 1-minute sustained winds of 230 km/h (145 mph). After stalling and executing a tight counter-clockwise loop near the coast, Gaemi slightly weakened due to land interaction before making landfall on the northeastern coast of Taiwan on 24 July. Gaemi accelerated as it moved across the island and emerged into the Taiwan Strait just six hours after making landfall. The system quickly weakened to a minimal tropical storm as it made its closest approach offshore of eastern China. Gaemi made final landfall at Xiuyu District of Putian in Fujian Province of China. Once inland, the system weakened to a tropical depression on 27 July. The above information was obtained from Wikipedia [26].

Damages from Typhoon Gaemi

Strong winds and heavy rainfalls during Typhoon Gaemi caused widespread flash flooding, landslide and damages to people and properties in the Philippines, Taiwan, China and Vietnam. Deaths and damages by country are provided in Table 3 [26].

Table 3: Deaths and damages from Typhoon Gaemi by country [26]

Country	Deaths	Damage cost
Philippines	48	$162.28 million
Taiwan	11	$88.8 million
China	49	$1.6 million
Vietnam	18	Unknown
Total	126	$253 million

Track and Data of Typhoon Gaemi

The track (route) of Typhoon Gaemi was obtained from [22, 27] and is shown in Figure 2. The cyclone data was obtained from IBTrACS [22]. The IBTrACS archived cyclone data contains 3 hourly information including date and time, track (path) and the maximum sustained wind speeds (1-minute mean).

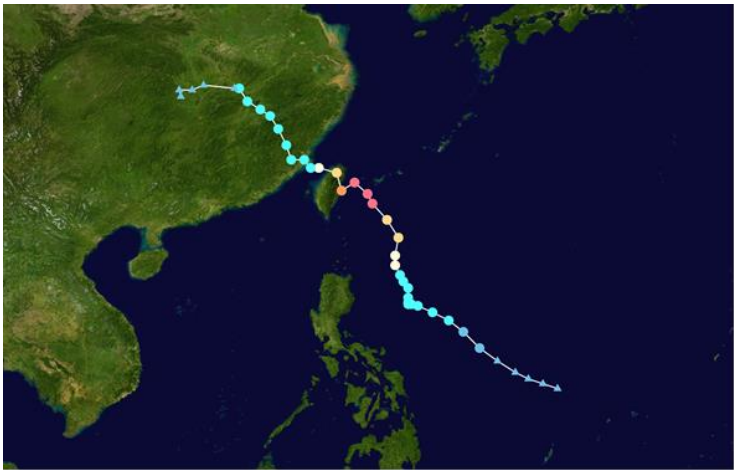

Figure 2a: Track of Typhoon Gaemi [27]

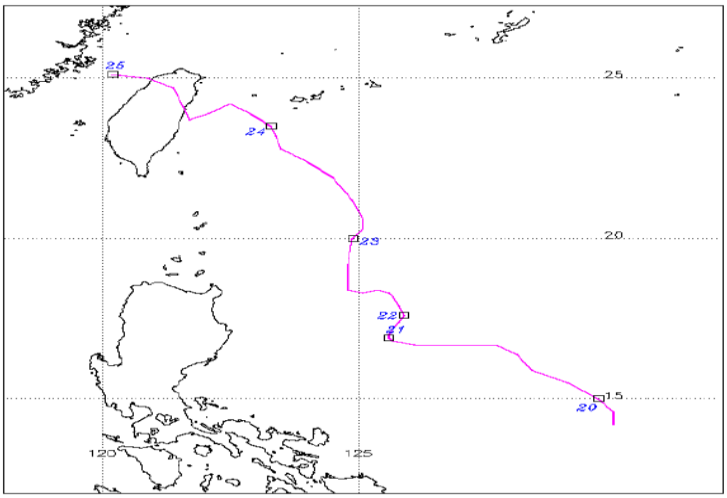

Figure 2b: *Track of Typhoon Gaemi [22]*

Data on Typhoon Gaemi is provided in Table 4 [22]. Figures 3, 4 and 5 show respectively the wind intensity, central pressure intensity and radial wind information for Typhoon Gaemi obtained from IBTrACS [22].

Table 4: Track and Data of the Typhoon Gaemi (2024) [22]

Date and Time [UTC]	Latitude [°N]	Longitude [°E]	Max 1-minute wind speeds [knots]	Central pressure [hPa]	Radius of maximum winds [nm]
19/07/2024 18:00	14.2	130.0	25	1003	48
19/07/2024 21:00	14.6	130.0	27	1003	48
20/07/2024 00:00	15.0	129.7	29	1002	48
20/07/2024 03:00	15.5	129.1	29	1002	50
20/07/2024 06:00	15.9	128.4	29	1002	52
20/07/2024 09:00	16.4	128.1	29	1002	50
20/07/2024 12:00	16.7	127.7	29	1001	48
20/07/2024 15:00	16.7	126.9	34	996	42
20/07/2024 18:00	16.7	126.1	39	991	35
20/07/2024 21:00	16.8	125.7	42	994	31
21/07/2024 00:00	16.9	125.6	45	996	26
21/07/2024 03:00	16.9	125.6	48	995	22
21/07/2024 06:00	16.8	125.7	51	993	17
21/07/2024 09:00	16.8	125.7	51	993	17
21/07/2024 12:00	16.9	125.6	51	992	17
21/07/2024 15:00	17.0	125.6	53	991	15
21/07/2024 18:00	17.2	125.7	54	989	12
21/07/2024 21:00	17.4	125.8	53	990	12
22/07/2024 00:00	17.6	125.9	51	991	12

22/07/2024 03:00	17.9	125.8	53	989	12
22/07/2024 06:00	18.2	125.7	54	986	12
22/07/2024 09:00	18.3	125.6	57	985	17
22/07/2024 12:00	18.4	125.4	60	984	22
22/07/2024 15:00	18.3	125.1	65	981	22
22/07/2024 18:00	18.4	124.8	70	977	22
22/07/2024 21:00	19.2	124.8	75	975	22
23/07/2024 00:00	20.0	124.9	80	973	22
23/07/2024 03:00	20.3	125.1	85	966	17
23/07/2024 06:00	20.6	125.1	89	959	12
23/07/2024 09:00	21.2	124.9	91	956	12
23/07/2024 12:00	21.9	124.5	93	952	12
23/07/2024 15:00	22.4	124.0	106	950	8
23/07/2024 18:00	22.8	123.5	119	948	4
23/07/2024 21:00	23.2	123.4	119	942	7
24/07/2024 00:00	23.5	123.3	119	935	10
24/07/2024 03:00	23.9	122.9	122	927	7
24/07/2024 06:00	24.2	122.5	124	919	4
24/07/2024 09:00	23.9	122.1	117	924	4
24/07/2024 12:00	23.7	121.7	109	928	4
24/07/2024 15:00	24.1	121.6	101	937	7
24/07/2024 18:00	24.7	121.4	93	945	9
24/07/2024 21:00	25.0	120.8	84	953	9
25/07/2024 00:00	25.1	120.2	74	961	9
25/07/2024 03:00	25.1	119.9	67	963	9
25/07/2024 06:00	25.2	119.8	60	964	9
25/07/2024 09:00	25.4	119.6	56	969	13
25/07/2024 12:00	25.6	119.4	51	973	17
25/07/2024 15:00	25.6	119.0	48	976	17
25/07/2024 18:00	25.6	118.6	45	978	17

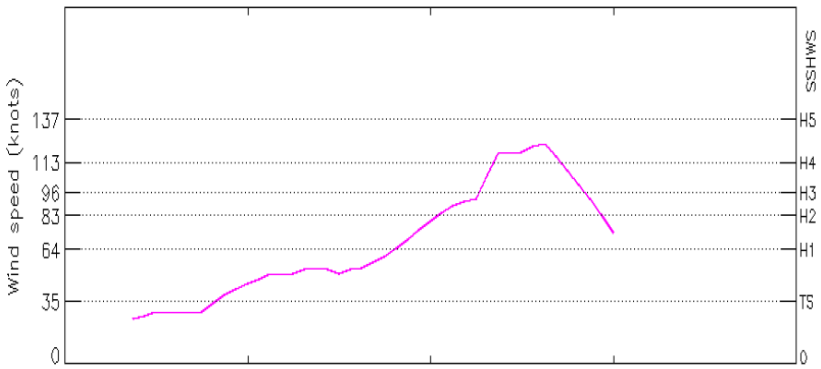

Figure 3: *Wind intensity plot [22]*

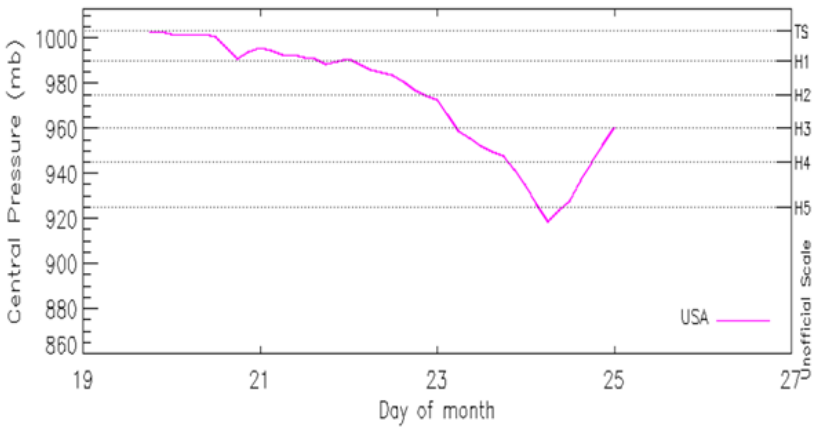

Figure 4: *Central pressure intensity plot [22]*

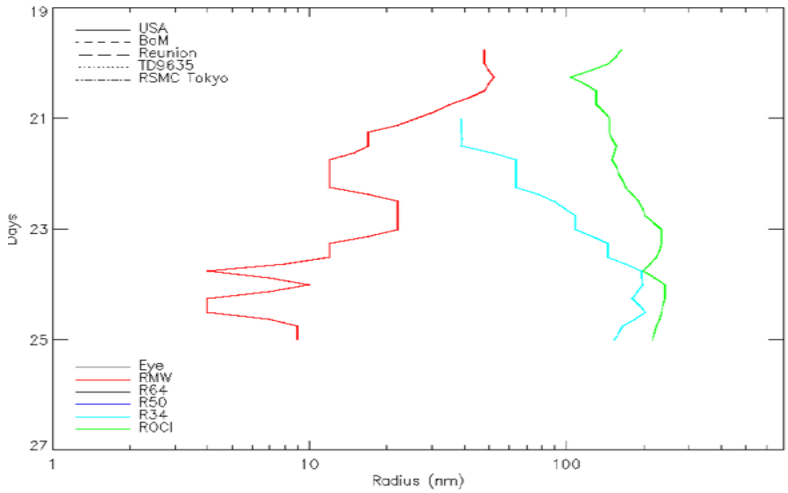

Figure 5: *Radial wind information [22]*

WIND AND PRESSURE FIELDS GENERATION

The MIKE21 Cyclone Wind Generation Tool developed by DHI [23] was used to generate the cyclonic wind and pressure fields for the passage of Typhoon Gaemi. The tool allows users to compute wind and pressure data due to tropical cyclones (hurricanes or typhoons). Several cyclone parametric models are included in the tool such as Young and Sobey model (1981) [28], Holland – single vortex model (1981), Holland – double vortex model (1980) [29] and Rankine vortex model. The Young and Sobey model (1981) [28] was used in the study. The Young and Sobey model (1981) [28] as below requires six input parameters (i.e., time, track, radius of maximum wind speed, maximum wind speed, central pressure, and neutral pressure). The other models require some additional parameters (such as Holland parameter B and Rankine parameter X) that need to be calculated using empirical relationships. This adds further uncertainty to the generated wind and pressure fields. Therefore, the other models were not used for the study.

It should be noted that the 1-minute mean wind speeds in Table 4 were converted into 1-hour mean using the methodology described in the World Meteorological Organisation (WMO) [30] for use in the Cyclone Wind Generation Tool. Usually, 1-hour mean wind speeds are used for numerical modelling of cyclone waves and surge.

According to Young and Sobey (1981) [28], the rotational wind gradient speed Vg at a distance r from the centre of the cyclone is given by:

$$V_g(r) = V_{max} \cdot \left(\frac{r}{R_{mw}}\right)^7 . exp\left(7\left(1 - \frac{r}{R_{mw}}\right)\right) \qquad \text{for } r < R_{mw}$$

$$V_g(r) = V_{max} . exp\left((0.0025R_{mw} + 0.05)\left(1 - \frac{r}{R_{mw}}\right)\right) \qquad \text{for } r \geq R_{mw}$$

Where, Rmw is the radius to maximum wind speed and Vmax is the maximum wind speed.

Following the Shore Protection Manual (1984) [31], the pressure p is given by:

$$p(r) = p_c + (p_n - p_c). exp\left(-\frac{R_{mw}}{r}\right)$$

Where, pc is the pressure at the storm centre or central pressure and pn is the ambient surroundings pressure field or neutral pressure.

Three types of wind corrections are available in the Cyclone Wind Generation Tool of DHI [23] to reflect the cyclonic wind structure. These wind corrections are described below from the Scientific Documentation of the Cyclone Wind

Generation Tool of DHI [23].

a) Geostrophic Correction

The parametric models usually provide wind information at the geo¬strophic or gradient wind level above the influence of the planetary boundary layer. This gradient wind speed (Vg) may be reduced to the standard surface reference level (V10) by considering the effects of the boundary layers as below:

$$V_{10}(r) = K_m . V_g(r)$$

Where, Vg(r) is the rotational gradient wind speed (m/s) at a distance r from the centre of the cyclone, V10 is the near-surface wind speed (m/s), and Km is the boundary layer wind speed correction coefficient.
Three options are available in the DHI tool [23], namely no correction, constant correction, and Harper et al. (2001) [32]. Harper et al. (2001) [32] empirical formulation was used in the present study where Km is dependent on Vg through a set of equa¬tions as below:

$$K_m = \begin{cases} 0.81 & for\ V_g < 6\ m/s \\ 0.81 - 2.96\ 10^{-3}(V_g - 6) & for\ 6 \le V_g < 19.5 \\ 0.77 - 4.31\ 10^{-3}(V_g - 19.5) & for\ 19.5 \le V_g < 45 \\ 0.66 & for\ V_g > 45\ m/s \end{cases}$$

b) Forward Motion Asymmetry

Cyclone winds circulate clockwise in the Southern Hemisphere. The wind field is asymmetric so that winds are typically stronger to the left of cyclone's track and lower to the right due to the contribution of the cyclone movement.
Two options are available in the DHI tool to consider the forward motion asymmetry at surface level, namely no correction and Harper et al. (2001) [32]. Harper et al. (2001) [32] empirical formulation (as below) was used in the present study where the user must specify the proportion of the cor¬rection factor, delta (δfm) and the angle of maximum winds, theta max (θmax). The proportion of the added forward cyclone speed (Vfm) can be adjusted using the correction factor delta (δfm). Theta max (θmax) is measured relative to the cyclone movement direction. In the DHI tool, the cyclone movement direction and the cyclone speed are computed based on the position of the centre of the storm given in the best track data table.

$$V_{10}(r,\theta) = K_m\,.V_g(r) + \delta_{fm}.V_{fm}.cos(\theta_{max} - \theta)$$

c) Inflow Angle

All the parametric wind models described earlier assume a circular wind flow pattern which does not represent the observed surface wind directions. Friction effects between water and air cause a deflection of the wind direction towards the centre of the cyclone. Two options are available in the DHI tool, namely no correction and Sobey et al. (1977) [33]. Sobey et al. (1977) [33] empirical formulation (as below) was used in the present study where the deflection is characterised by the inflow angle (β) in the order of 25° but decreases towards the storm centre.

$$\beta = \begin{cases} 10\,\dfrac{r}{R_{mw}} & \text{for } 0 \le r < R_{mw} \\ 10 + 75\left(\dfrac{r}{R_{mw}} - 1\right) & \text{for } R_{mw} \le r < 1.2\,R_{mw} \\ 25 & \text{for } r \ge 1.2\,R_{mw} \end{cases}$$

RESULTS AND DISCUSSIONS

Two-dimensional wind and pressure fields were generated along the entire path of Typhoon Gaemi. Then two-dimensional wind and pressure fields at key selected locations were extracted. These locations are shown in Figure 6. Coordinates, hourly timesteps and date and time of these locations are provided in Table 5.

Table 5: Wind and pressure fields extraction locations, timesteps and date and time

Locations	Coordinates		Hourly timesteps	Date and time
	Latitude (°N)	Longitude (°E)		
P1	16.9	125.6	30	21/07/2024 00:00
P2	18.4	124.8	72	22/07/2024 18:00
P3	24.2	122.5	108	24/07/2024 06:00
P4	23.7	121.7	114	24/07/2024 12:00
P5	24.7	121.4	120	24/07/2024 18:00
P6	25.1	120.2	126	25/07/2024 00:00
P7	25.2	119.8	132	25/07/2024 06:00

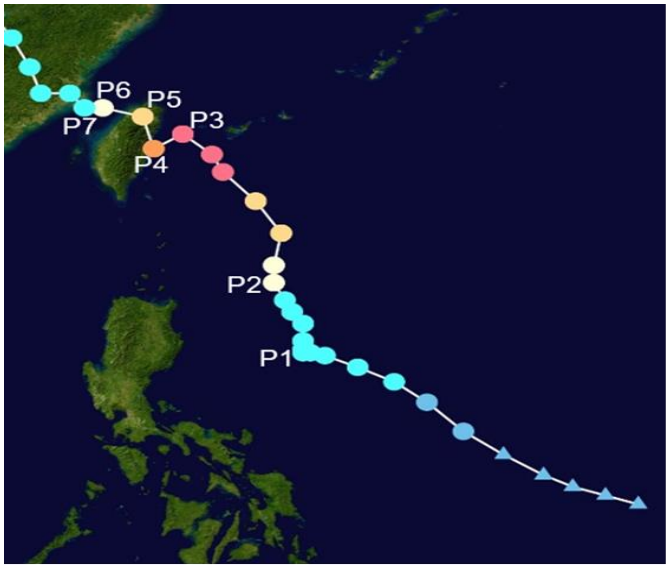

Figure 6: *Wind and pressure fields extraction locations*

The top plot in Figures 7 to 13 show the two-dimensional wind fields when the typhoon reached to locations P1 to P7 respectively. Time-series of wind speeds at these locations during the entire passage of the typhoon are presented at bottom of these figures. Figure 14 compares the time-series of wind speeds at the selected locations during the entire passage of the typhoon.

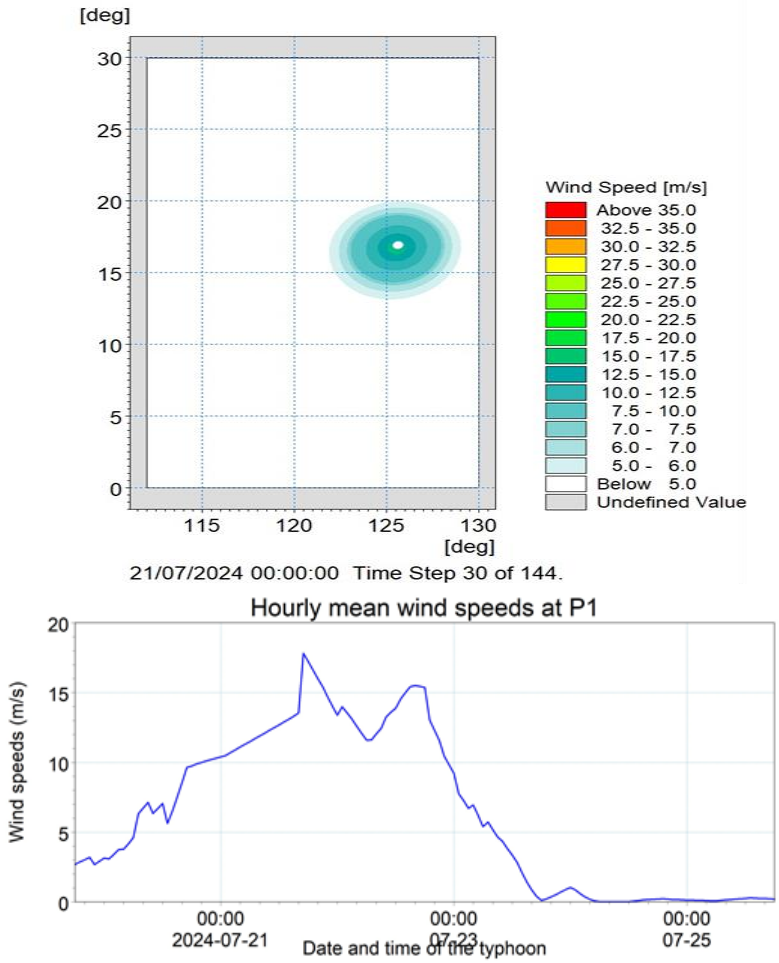

Figure 7: *Wind field of Typhoon Gaemi at P1 (top – 2D wind field; bottom – time-series of wind speeds)*

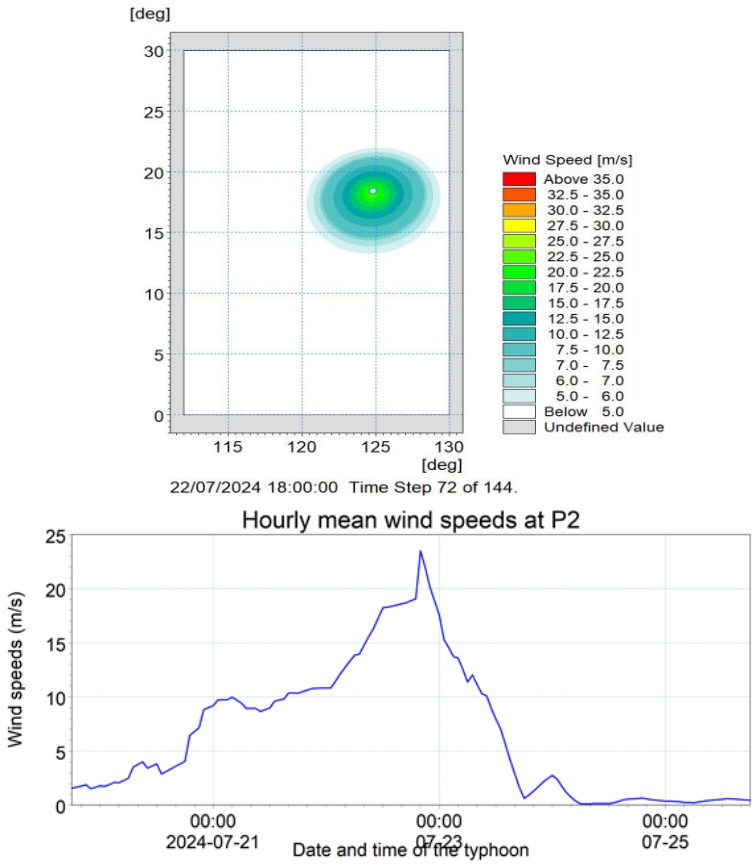

Figure 8: *Wind field of Typhoon Gaemi at P2 (top – 2D wind field; bottom – time-series of wind speeds)*

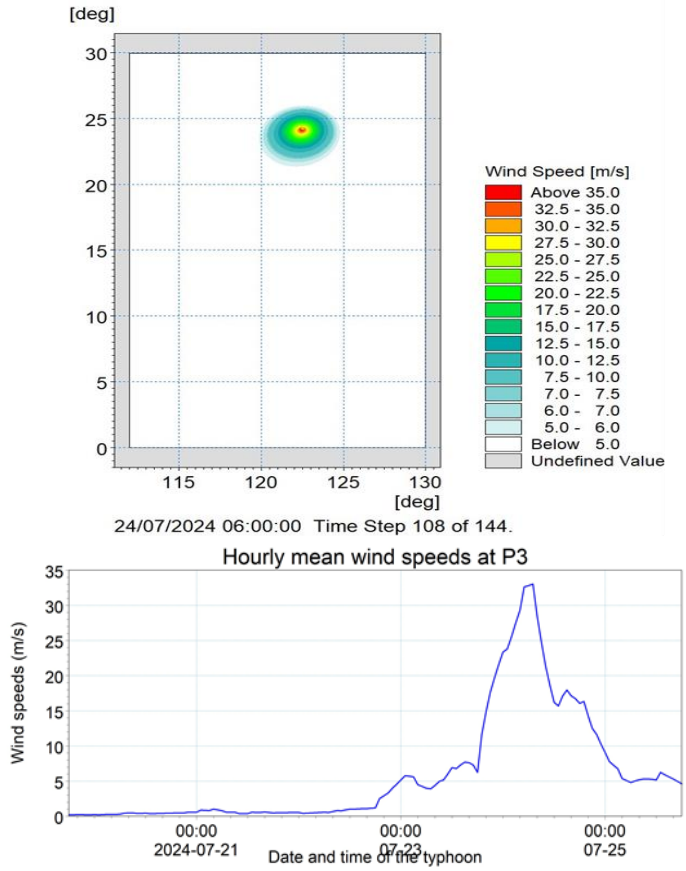

Figure 9: *Wind field of Typhoon Gaemi at P3 (top – 2D wind field; bottom – time-series of wind speeds)*

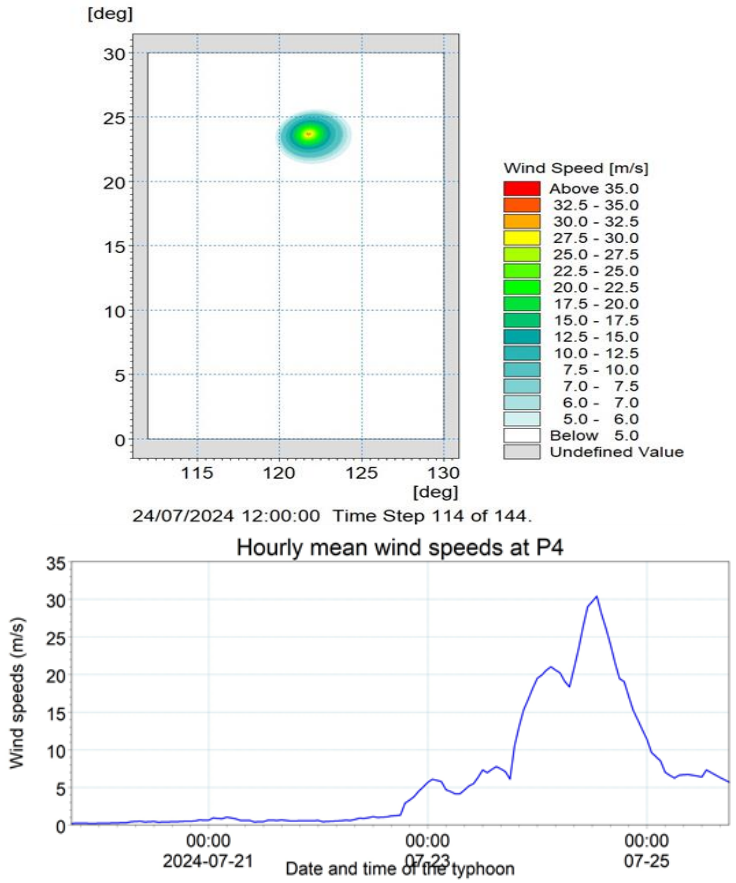

Figure 10: *Wind field of Typhoon Gaemi at P4 (top – 2D wind field; bottom – time-series of wind speeds)*

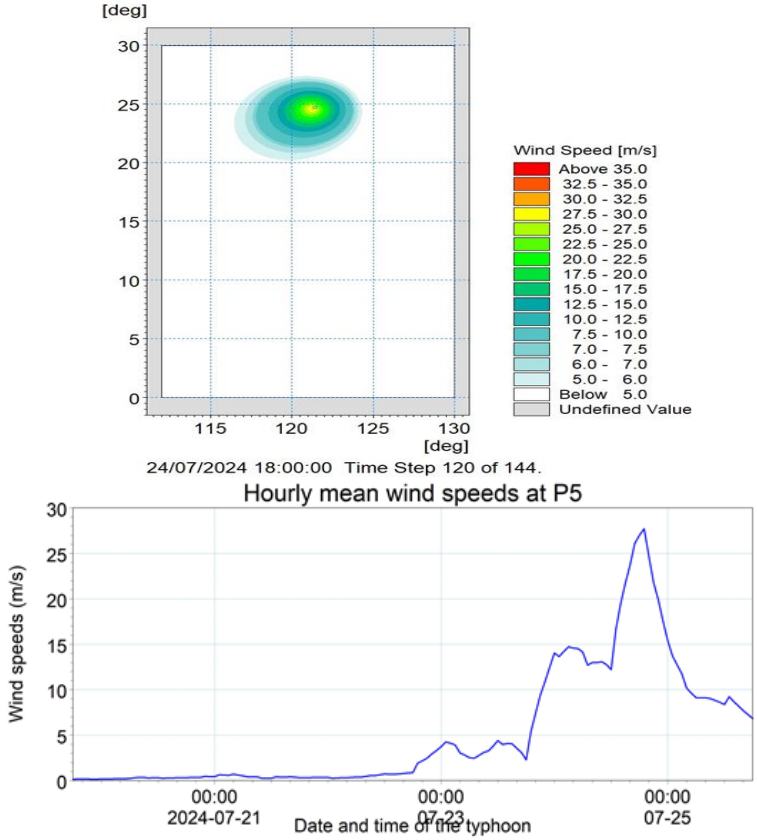

Figure 11: *Wind field of Typhoon Gaemi at P5 (top – 2D wind field; bottom – time-series of wind speeds)*

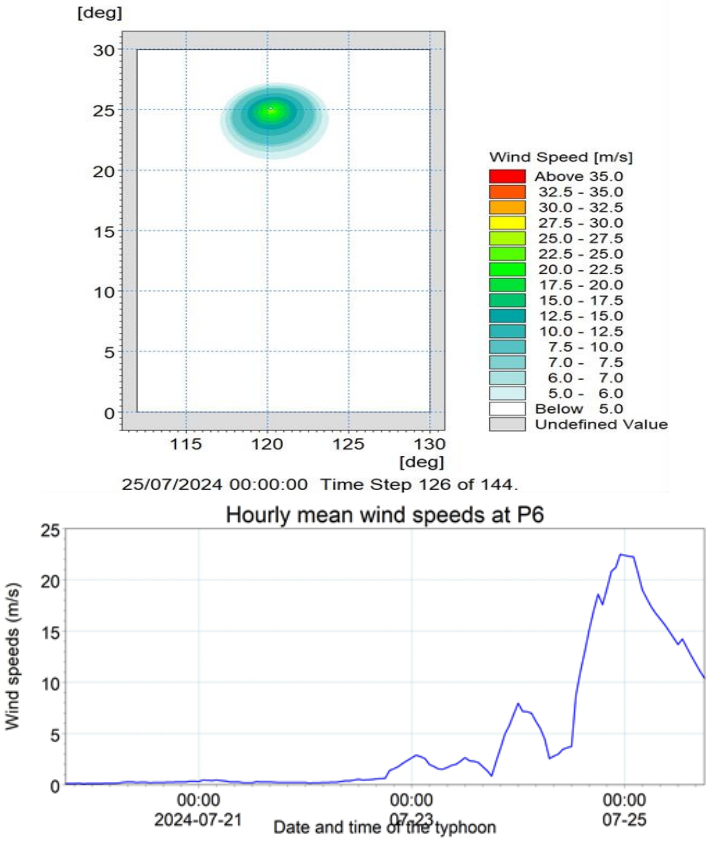

Figure 12: *Wind field of Typhoon Gaemi at P6 (top – 2D wind field; bottom – time-series of wind speeds)*

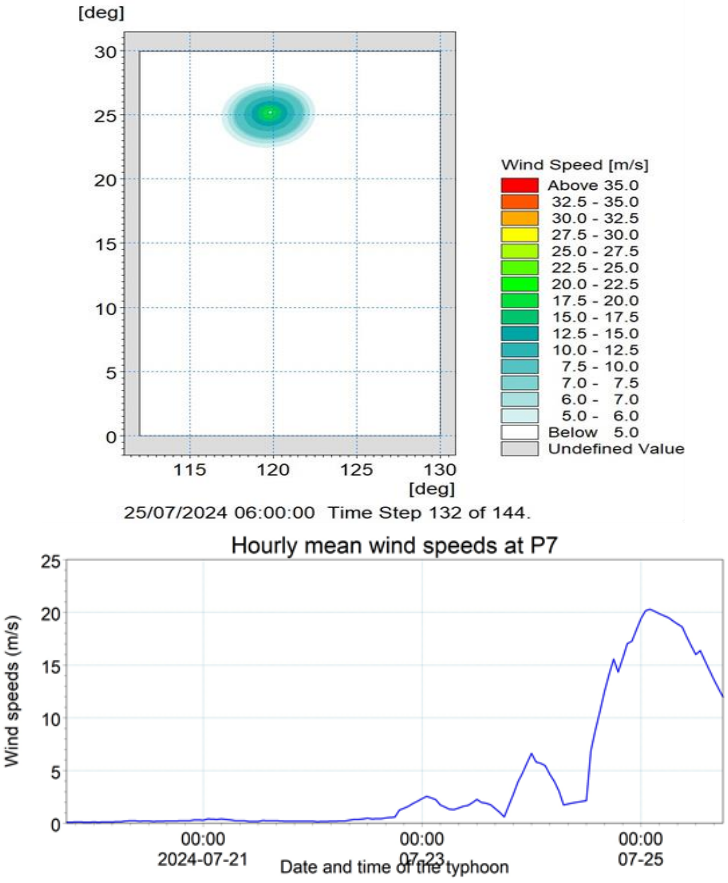

Figure 13: *Wind field of Typhoon Gaemi at P7 (top – 2D wind field; bottom – time-series of wind speeds)*

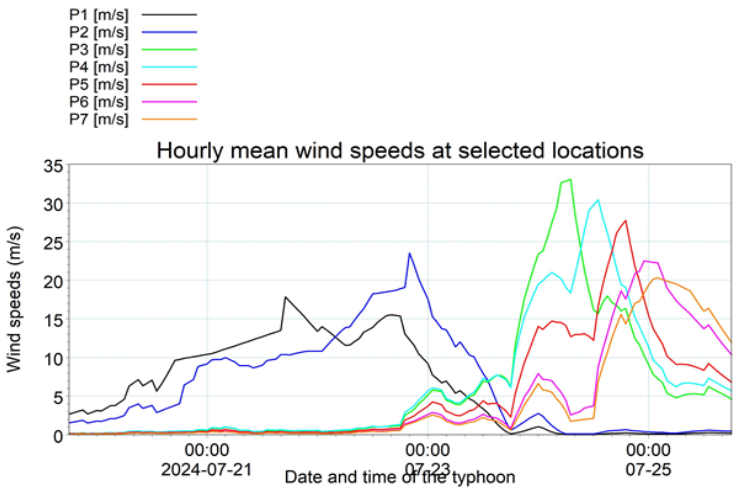

Figure 14: *Time-series of hourly-mean wind speeds at the selected locations during the entire passage of Typhoon Gaemi*

The top plot in Figures 15 to 21 show the two-dimensional pressure fields when the typhoon reached to locations P1 to P7 respectively. Time-series of pressure at these locations during the entire passage of the typhoon are presented at bottom of these figures. Figure 22 compares the time-series of pressure at the selected locations during the entire passage of the typhoon.

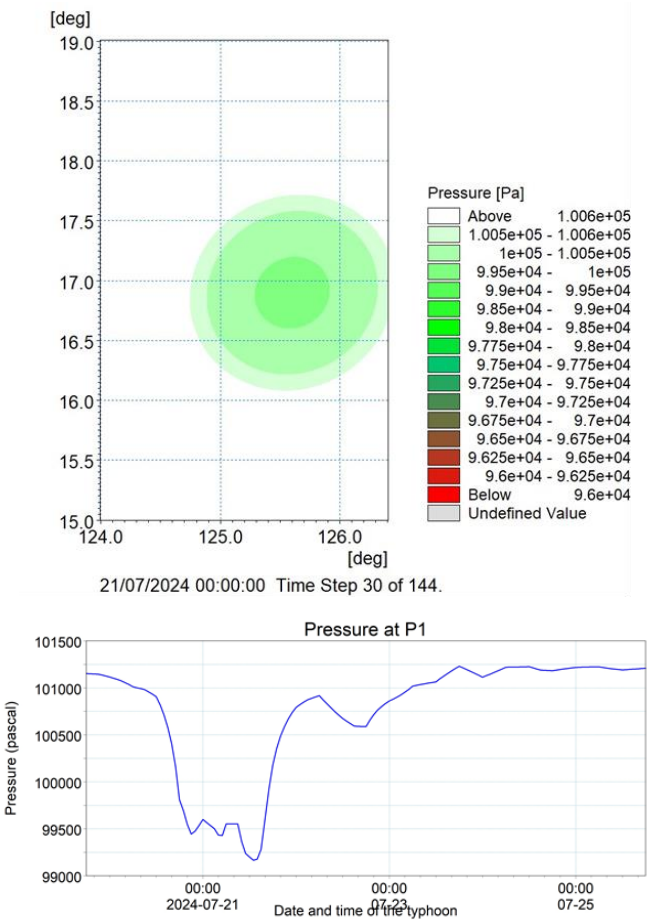

Figure 15: *Pressure field of Typhoon Gaemi at P1 (top – 2D pressure field; bottom – time-series of pressure)*

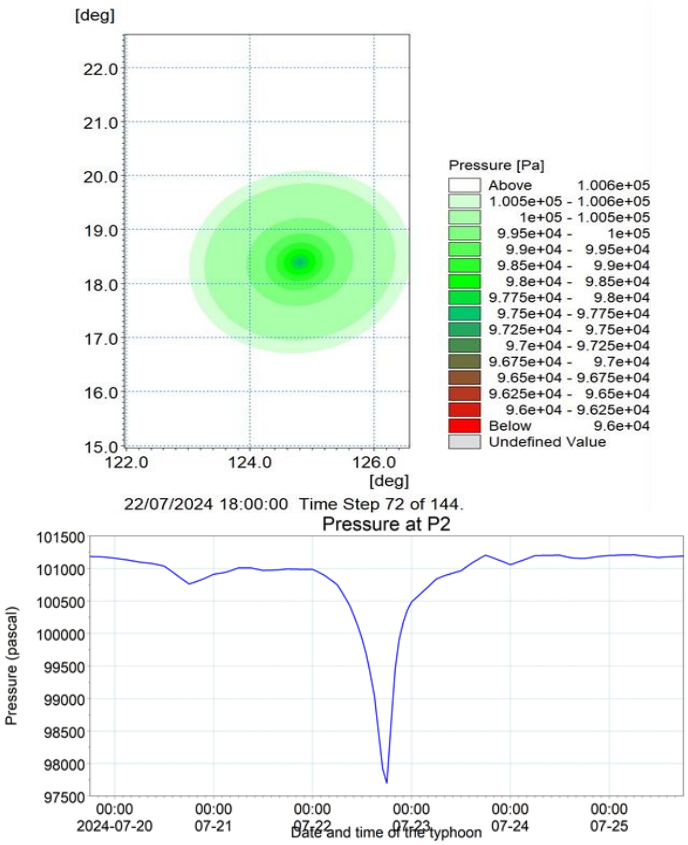

Figure 16: *Pressure field of Typhoon Gaemi at P2 (top – 2D pressure field; bottom – time-series of pressure)*

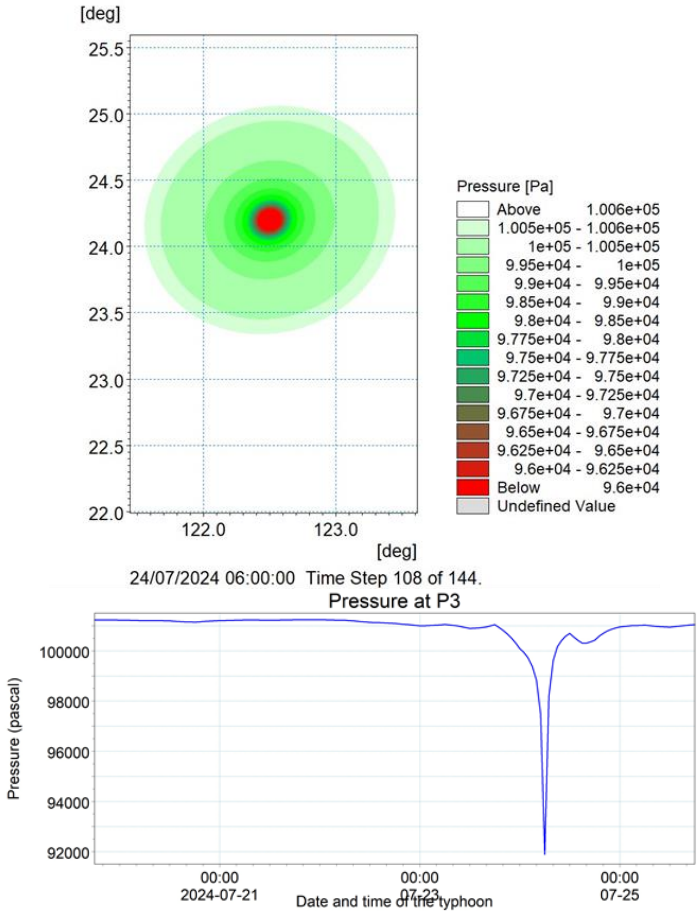

Figure 17: *Pressure field of Typhoon Gaemi at P3 (top – 2D pressure field; bottom – time-series of pressure)*

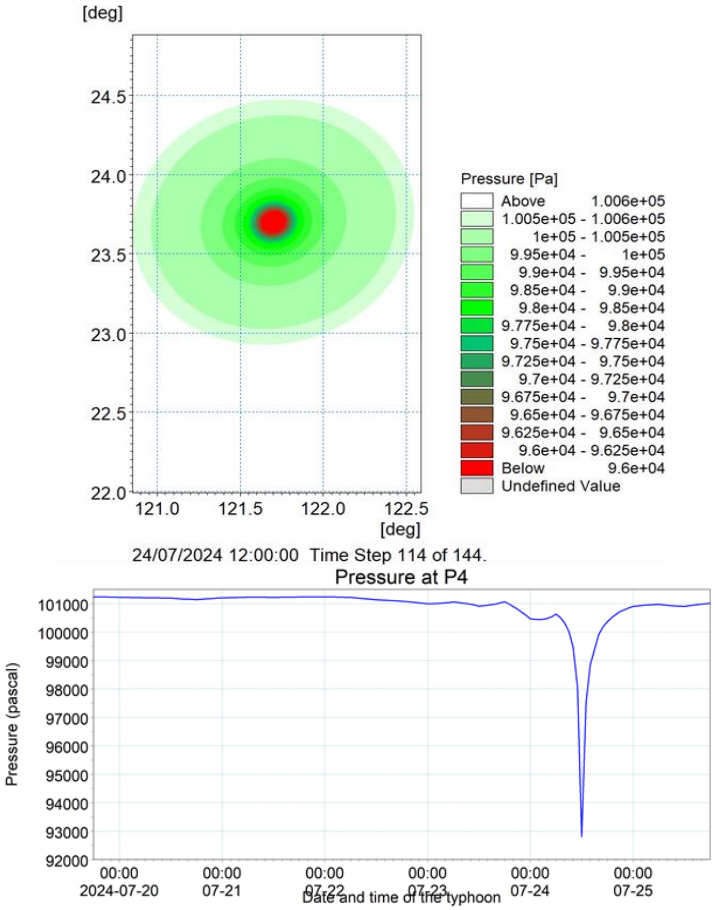

Figure 18: *Pressure field of Typhoon Gaemi at P4 (top – 2D pressure field; bottom – time-series of pressure)*

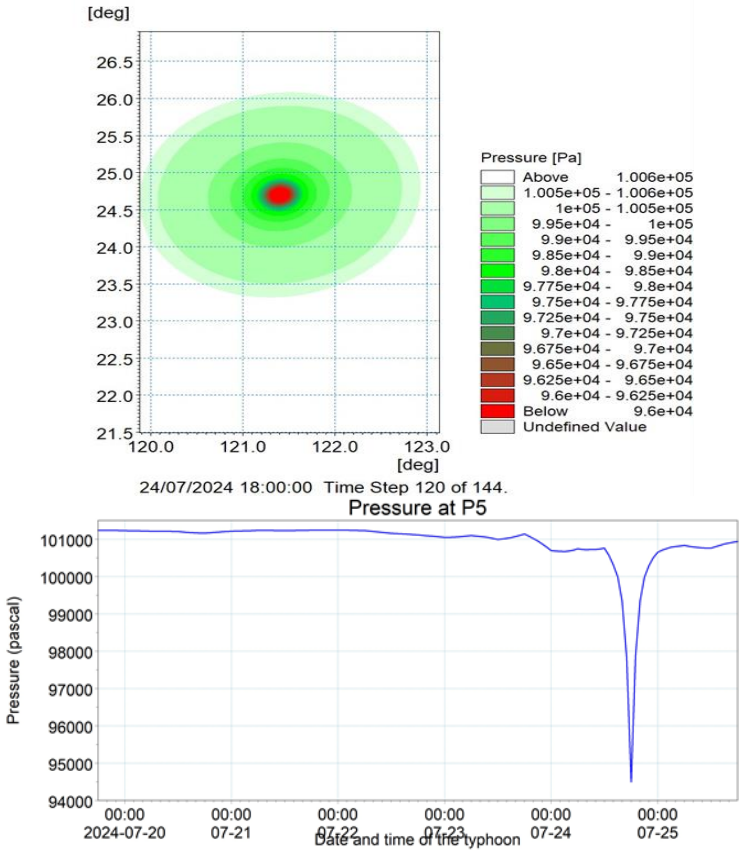

Figure 19: *Pressure field of Typhoon Gaemi at P5 (top – 2D pressure field; bottom – time-series of pressure)*

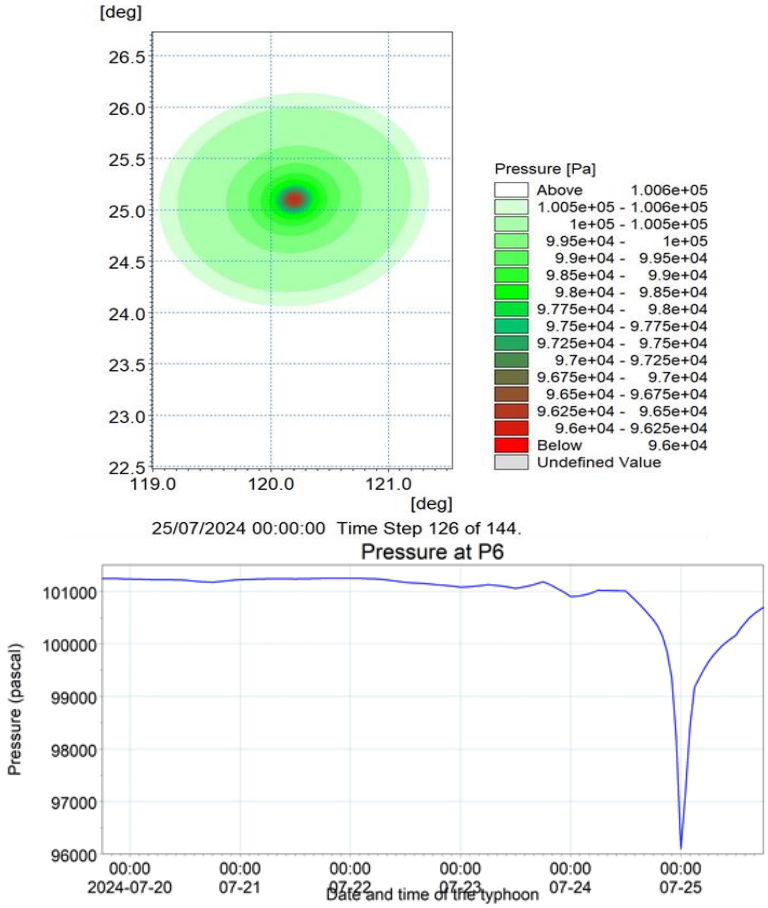

Figure 20: *Pressure field of Typhoon Gaemi at P6 (top – 2D pressure field; bottom – time-series of pressure)*

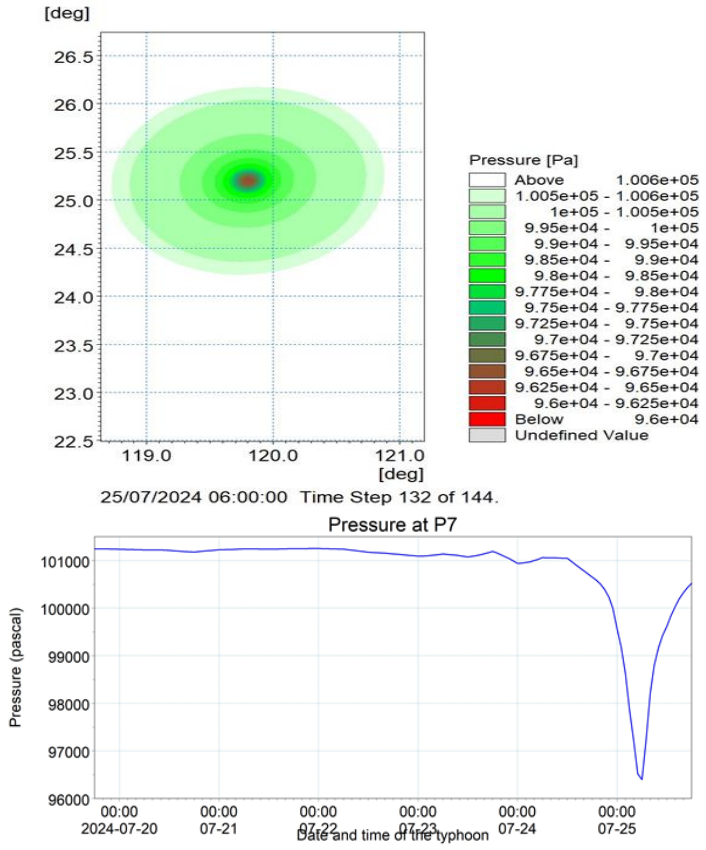

Figure 21: *Pressure field of Typhoon Gaemi at P7 (top – 2D pressure field; bottom – time-series of pressure)*

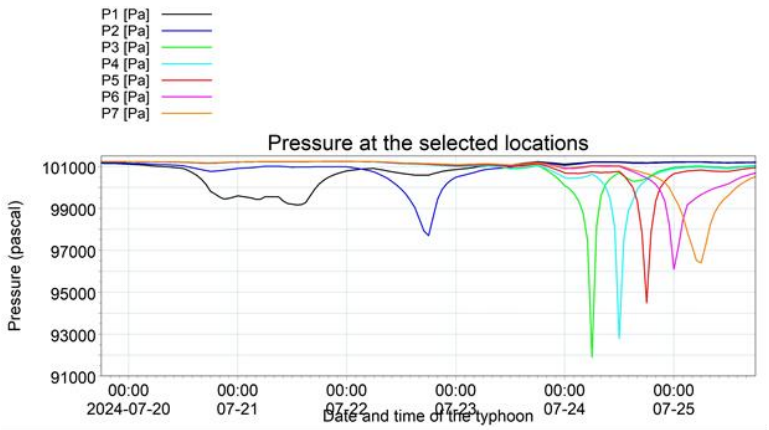

Figure 22: *Time-series of pressure at the selected locations during the entire passage of Typhoon Gaemi*

The highest wind speeds and the lowest pressures at the selected locations during the entire passage of Typhoon Gaemi are summarised in Table 6 from the time-series plots and are also shown in Figure 23. The highest wind speed and the lowest pressure are found in P3 where the typhoon reached to its peak intensity. It should be noted that 1 hPa = 100 Pascals (Pa).

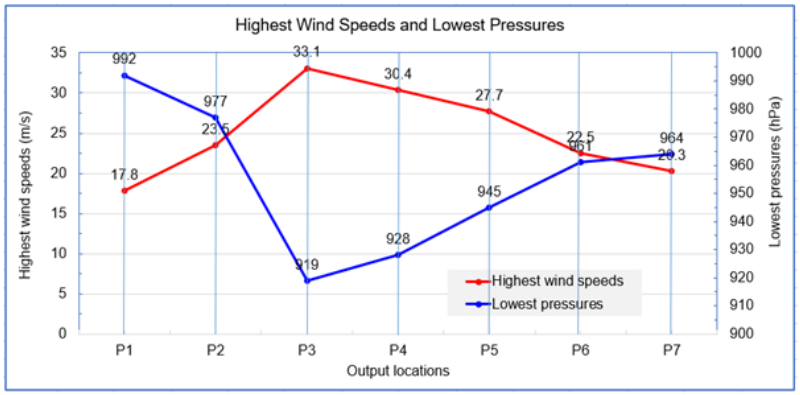

Figure 23: *Highest wind speeds and lowest pressures during Typhoon Gaemi at the selected locations extracted from the time-series plots*

Table 6: The highest wind speeds and the lowest pressures at the selected locations

Locations	Highest wind speed (m/s)	Lowest pressure (hPa)
P1	17.8	992
P2	23.5	977
P3	33.1	919
P4	30.4	928
P5	27.7	945
P6	22.5	961
P7	20.3	964

RECOMMENDED DESIGN CONSIDERATIONS

The potential impact of a cyclone event on the design of coastal and marine facilities may be summarised as follows:

1. Shoaling results in an increase in water levels and stronger currents inshore. Measures will be required to protect structures from scouring of the foreshore and seabed and limit damage to the crest if heavy overtopping occurs;
2. The foreshore will be subjected to flooding as the cyclone waves and surge approach; and
3. Facilities located on the landward slope are at risk from cyclone wave run-up and surge.

TYPHOON RISK REDUCTION MEASURES

Risks Reduction from Typhoons

Damage due to a cyclone depends on the strength and proximity of the cyclone as well as local bathymetry and topography and the location of people, structures, and facilities.

It is almost impossible to fully protect people and settlements from major cyclonic events. However, various soft and hard measures (independently or in combination) could be adopted to reduce fatalities and damage to key infrastructure.

Some potential measures to reduce the risk of damage and deaths from major cyclonic events are highlighted below:

1. Detection, early warning systems and real-time observation systems are of great importance;
2. Appropriate awareness and understanding among the general public;
3. Mitigation plans and evacuation and rescue preparedness by responsible authorities;
4. Cyclone risk assessment, flood risk and inundation hazard maps;
5. Cyclone shelters;
6. Developing artificial forest such as mangroves and casuarinas of appropriate width behind the shoreline to reduce cyclone wave energy;
7. Maintaining natural sand dunes;
8. Regulations for development in the coastal zone;
9. Saline embankments to prevent salt-water entering into fertile lands;
10. Raising ground levels of important structures and facilities such as warehouses, terminals and quays; and
11. Constructing cyclone defence structures such seawalls, dykes, gates, nearshore breakwaters, and offshore barriers. However, these structures are substantial and very expensive.

For major coastal infrastructure, the adoption of appropriate design parameters, a proper assessment of structural loads, forces, and stability in combination with a detailed understanding of cyclone processes will reduce the level of damage resulting from these events. Furthermore, physical modelling of major coastal and marine structures and mooring systems to investigate their stability under severe conditions will be helpful to reduce damage due to cyclones.

Risks Reduction from Mudslides and Landslides

High tides and heavy and prolonged rains during a cyclone may cause floods and submergence of low-lying areas which may lead to mudslides and landslides in mountainous areas causing loss of life and property. Landslides and mudslides are downhill earth movements that move slowly and cause gradual damage. They can also move rapidly destroying property and taking lives suddenly and unexpectedly. They typically carry heavy debris such as trees and boulders which cause severe damage together with injury or death. Faster movement of mudslides makes them deadly.

It is not possible to prevent a mudslide or a landslide. However, preparatory steps can be taken to lessen the impact of a mudslide. Some guidelines are briefly mentioned below:

1. Carrying out risk assessment;
2. Creating public awareness and practicing an evacuation plan;
3. Staying up to date on storm/rainfall/cyclone warnings during times of increased risk;
4. Watching for any visible signs such as cracks on land, debris flows or trees tilting or boulders knocking;
5. Staying alert and awake;
6. Moving out of the path of the landslide or debris flow; and
7. Some erosion control measures might be helpful (such as installing barrier walls, improving drainage system and planting trees with deep and extensive root systems).

SUMMARY AND FINDINGS

Typhoon Gaemi, known in the Philippines as Super Typhoon Carina, was a powerful tropical cyclone that impacted East China after severely affecting Taiwan and the Philippines in late July 2024. This paper has focused to Typhoon Gaemi as less information is available on this event.

Raw data (such as track, wind speed, pressure, and radius of maximum wind speed) have been obtained from IBTrACS [22]. Two-dimensional wind and pressure fields along the entire track were then generated using the Cyclone Wind Generation Tool developed by DHI [23].

Two-dimensional wind and pressure fields at selected locations along the track are presented in this paper. Time-series wind speed and pressure during the entire passage of the typhoon are also provided at these selected locations.

The highest wind speeds and the lowest pressures at the selected locations are summarised both in tabular and graphical formats from the time-series plots at these locations. The highest wind speed and the lowest pressure are found in P3 where the typhoon reached to its peak intensity.

The two-dimensional wind and pressure fields will be useful for numerical modelling of waves and surge. Structural design considerations and cyclone risk reduction measures are also described in this paper. The methodology described in this paper for generating wind and pressure fields from Typhoon Gaemi could also be applied for other typhoons around the world.

ACKNOWLEDGEMENTS

The author would like to thank Royal HaskoningDHV (an independent, international engineering and project management consultancy company, www.royalhaskoningdhv.com) for giving permission to publish this paper. The author would like to thank his colleague Debra Griffin for carrying out the proof reading of this manuscript. The author would also like to thank the external reviewers who provided valuable comments to improve the paper.

REFERENCES

[1]. Simpson, R. H. (1974). The hurricane disaster--potential scale. Weatherwise, 27, 169. https://www.aoml.noaa.gov/general/WWW000/text/sfsimp.html.https://www.aoml.noaa.gov/hrd/Landsea/deadly/Table1.htm.

[2]. Adler, R. F. (2005). Estimating the benefit of TRMM tropical cyclone data in saving lives, June 20, 2005.

[3]. Ubydul Haque, Masahiro Hashizume, Korine N Kolivras, Hans J Overgaard, Bivash Das, and Taro Yamamotoa (2012). Reduced death rates from cyclones in Bangladesh: what more needs to be done? Bulletin of the World Health Organization, 2012 Feb 1; 90(2): 150-156, PMCID: PMC3302549, published online 2011 Oct 24. doi: 10.2471/BLT.11.088302.

[4]. Arizona State University (2020). World: Highest Mortality, Tropical Cyclone. World Meteorological Organization's World Weather & Climate Extremes Archive. Arizona State University, November 12, 2020.

[5]. Business Insider India (2017). The 16 deadliest storms of the last century, Business Insider India, September 13, 2017.

[6]. Julian, F. (2019). Remembering the great Bhola cyclone, Dhaka Tribune, November 9, 2019.

[7]. Rudolph, D. K. and Guard, C. P. (1992). 1991 Annual Tropical Cyclone Report. U.S. Naval Oceanography Command Center, Joint Typhoon Warning Center, https://web.archive.org/web/20200813232009/https://www.usno.navy.mil/NOOC/nmfc-ph/RSS/jtwc/atcr/1991atcr.pdf.

[8]. United States Agency for International Development. The Bangladesh Cyclone of 1991 (PDF) (Report), United States Agency for International Development, https://pdf.usaid.gov/pdf_docs/Pnadg744.pdf.

[9]. WMO (2020). World's deadliest tropical cyclone was50 years ago. World Meteorological Organization (WMO), Tags: Tropical cyclones, Disaster risk reduction, published 12 November 2020, member Bangladesh, https://wmo.int/media/news/worlds-deadliest-tropical-cyclone-was-50-years-ago.

[10]. Dunn, G., E. (1962). The tropical cyclone problem in East Pakistan. Mon. Wea. Rev., 91, 83-86.

[11]. Frank, Neil and Husain, S. A. (1971). The deadliest tropical cyclone in history? Bulletin of the American Meteorological Society. American Meteorological Society, volume 52, number 6, page 438-444, June 1971. Bibcode:1971BAMS...52..438F. doi:10.1175/1520-0477(1971)052<0438:TDTCIH>2.0.CO;2.

[12]. de la Cruz, Gwen (2016). IN NUMBERS: Typhoons in the Philippines and the 2016 polls (19 March 2016). Rappler. Retrieved April 12, 2017.

[13]. Brown, Sophie (2013). The Philippines Is the Most Storm-Exposed Country on Earth (11 November 2013). Time. Retrieved April 12, 2017.

[14]. García-Herrera, Ricardo; Ribera, Pedro; Hernández, Emiliano; Gimeno, Luis (2003). Typhoons in the Philippine Islands, 1566–1900 (PDF) (26 September 2003). David V. Padua. p. 40. Retrieved April 13, 2010.

[15]. Overland, Indra et al. (2017). Impact of Climate Change on ASEAN International Affairs: Risk and Opportunity Multiplier, Norwegian Institute of International Affairs (NUPI) and Myanmar Institute of International and Strategic Studies (MISIS).

[16]. Relief International Inc (2024). Relief International Inc, 1101 14th St., NW, Suite 710, Washington, D.C. 20005, United Sates. https://www.ri.org/countries/philippines?gad_source=1&gclid=EAIaIQobChMIloy4stDnhwMVhJRQBh28NibjEAAYAyAAEgJxJ_D_BwE.

[17]. Citynoise at English Wikipedia (2008). Tropical Cyclones, 1945–2006. Data from the Joint Typhoon Warning Center and the U.S. National Oceanographic and Atmospheric Administration. Colors based on Template talk: Storm colour. By Citynoise at English Wikipedia, CC BY-SA 3.0, March 2008. https://commons.wikimedia.org/w/index.php?curid=18049077.

[18]. Wikipedia (2024a). Typhoons in the Philippines. https://en.wikipedia.org/wiki/Typhoons_in_the_Philippines.

[19]. Del Rosario, Eduardo D [2011]. Final Report on Typhoon "Yolanda" (Haiyan) (PDF) (Report). Philippine National Disaster Risk Reduction and Management Council. pp. 77–148, 9 August 2011. Archived (PDF) from the original on November 5, 2020. Retrieved March 27, 2022.

[20]. del Rosario, Eduardo D. [2014]. FINAL REPORT Effects of Typhoon YOLANDA (HAIYAN) (PDF) (Report). NDRRMC, April 2014. Retrieved March 14, 2015.

[21]. Paulhaus, J. L. H. [1973]. World Meteorological Organization Operational Hydrology Report No. 1: Manual for Estimation of Probable Maximum Precipitation. World Meteorological Organization, 1973, p. 178.
[22]. IBTrACS (2024). Super Typhoon GAEMI. International Best Track Archive for Climate Stewardship (IBTrACS). https://ncics.org/ibtracs/index.php?name=v04r01-2024202N14130.
[23]. DHI (2024). MIKE21 Cyclone Wind Generation Tool, Scientific Documentation, DK-2970, Hørsholm, Denmark, 2024.
[24]. JMA (2024). The Japan Meteorological Agency, Ministry of Land, Infrastructure, Transport and Tourism. https://www.jma.go.jp/jma/indexe.html.
[25]. JTWC (2024). Joint Typhoon Warning Center, A Joint United States Navy – United States Air Force command in Pearl Harbor, Hawaii. https://www.metoc.navy.mil/jtwc/jtwc.html.
[26]. Wikipedia (2024b). Typhoon Gaemi. https://en.wikipedia.org/wiki/Typhoon_Gaemi.
[27]. Wikipedia (2024c). Typhoon Gaemi. https://en.wikipedia.org/wiki/Typhoon_Gaemi. [Track created by Meow using Wikipedia: WikiProject Tropical cyclones/Tracks. The background image is from NASA. Tracking data is from NOAA and JMA. https://en.wikipedia.org/wiki/Typhoon_Gaemi#/media/File:Gaemi_2024_path.png].
[28]. Young, I.R. and Sobey, R.J. (1981). The numerical prediction of tropical cyclone wind-waves. James Cook University of North Queensland, Townville, Dept. of Civil & Systems Eng., Research Bulletin No. CS14.
[29]. Holland, G. (1980). An analytic model of the wind and pressure profiles in hurricanes. Monthly weather review, volume 108, pp. 1212-1218.
[30]. WMO (2008). Guidelines for converting between various wind averaging periods in tropical cyclone conditions, Appendix II, World Meteorological Organisation (WMO), October 2008.
[31]. Shore Protection Manual (1984). Department of the Army, US Army Corps of Engineers, Washington, DC 20314.
[32]. Harper, B.A., Hardy, T.A., Mason, L.B., Bode, L., Young, I.R., Nielsen, P. (2001). Queensland climate change and community vulnerability to tropical cyclones. Ocean Hazards Assessment – Stage 1, Report, Department of Natural Resources and Mines, Queensland, Brisbane, Australia, 368 p.
[33]. Sobey, R.J., Harper, B.A. and Stark, K.P. (1977). Numerical simulation of tropical cyclone storm surge. Research Bulletin CS-14, Dept Civil and Systems Engineering, James Cook University.